

Robust Optimization for IMPT: Introducing and Comparing Different Automated Approaches

Joana Neves[1], Humberto Rocha[1,2(✉)], Brígida Ferreira[2,3], and Joana Dias[1,2]

[1] University of Coimbra, INESC-Coimbra, 3030-290 Coimbra, Portugal
{hrocha,joana}@fe.uc.pt
[2] University of Coimbra, CeBER, FEUC, 3004-512 Coimbra, Portugal
[3] University of Lisbon, IBEB, Faculty of Sciences, 1749-016 Lisbon, Portugal
bcferreira@fc.ul.pt

Abstract. Intensity-modulated proton therapy (IMPT) is a radiotherapy treatment modality that has proven to be able to properly irradiate tumors while preserving as much as possible normal tissues. However, it is extremely vulnerable to several different sources of uncertainties, which motivates the use of robust treatment planning optimization. In this work we describe a new approach for robust automated IMPT treatment optimization, based on a set of auxiliary structures that are shifted versions of each one of the volumes of interest (clinical target volume - CTV and organs-at-risk - OARs), and that are named *clones*. This approach is compared with the use of a pseudo-Planning Target Volume (PTV) and pseudo-planning OAR volumes built by the union of all the CTV and OAR *clones*, respectively. For proof-of-concept, the proposed methodologies were tested using five post-operative prostate cancer cases. The quality of the calculated treatment plans was assessed by Monte Carlo simulation. For IMPT treatment plan robust optimization, the new strategy based on the use of *clones* using shifts of 6 mm presented better results in terms of robustness when compared with the traditional PTV-based approach. Taking uncertainties into consideration during the planning process can be an option to overcome one of the major drawbacks of IMPT.

Keywords: automated treatment planning · inverse optimization · Monte Carlo simulation · radiotherapy · robust optimization

1 Introduction

Several therapeutic modalities can be used for the treatment of cancer, namely surgery, chemotherapy, radiotherapy, among others. Radiotherapy is prescribed to most patients, many times in combination with surgery or chemotherapy [1]. Radiotherapy emerges as a form of oncological treatment that uses ionizing

© The Author(s), under exclusive license to Springer Nature Switzerland AG 2024
O. Gervasi et al. (Eds.): ICCSA 2024 Workshops, LNCS 14816, pp. 324–340, 2024.
https://doi.org/10.1007/978-3-031-65223-3_22

radiation to damage tumor cells. The aim is to deliver the prescribed dose of radiation to the tumor while minimizing the risk of side effects to healthy organs [2]. It can be delivered for therapeutic or palliative purposes, in order to alleviate the symptoms of patients. Highly sophisticated radiation therapy techniques have emerged in the last decades with the potential to deliver more conformal and homogeneous doses to the target volume, while better sparing the surrounding healthy tissues [3–5]. Intensity-modulated proton therapy (IMPT) is one of these techniques [5]. The physical properties of protons enable dose distributions that are conformal and homogeneous to the target volume, and, simultaneously, deposit less dose in organs at risk. Proton beams deposit maximum energy in a very precise location, called the Bragg peak, which contributes to the delivery of a dose distribution conformal to the target volume while keeping a low dose in the normal tissues. Consequently, there is the potential for an increase in tumor control probability as well as a decrease in the risk of secondary effects that occur by using ionizing radiation. However, one of the major drawbacks of IMPT is its higher susceptibility to uncertainties, such as the range of proton beams or patient positioning [6]. Therefore, it is essential to assure that treatment plans are robust, meaning that they are clinically admissible even under different scenarios that can occur [7].

When the medical oncologist prescribes an IMPT treatment, a set of procedures are put in place. First, it is necessary to acquire medical images of the patient, usually a computed tomography scan (CT), where all the volumes of interest are delineated. These volumes represent the tumor (clinical target volume - CTV) and also all the organs that must be spared (Organs-at-risk - OARs). These medical images create a 3D discretization of the patient, with the smallest 3D-element called a voxel. Then the oncologist defines the medical prescription, that establishes a set of upper or lower limits to some dosimetric measures associated with each volume of interest. For CTVs these limits will make sure that the volume is properly irradiated. For OARs, upper limits to the deposited dose are usually considered, depending on the characteristics of the organs, trying to assure that all the organs keep their functionality. Then the treatment planner goes through a lengthy and complex trial-and-error process, calculating different treatment plans iteratively until one treatment plan is found that complies with all the constraints defined in the medical prescription. This process is usually known as inverse optimization treatment planning and it is based on the use of optimization models and algorithms. The planner changes some of the parameters of an optimization model, that is solved producing a new treatment plan. Most of the time this inverse optimization procedure is interpreted by the planner as a black box, with which the planner can only interact by changing some parameters, but without knowing what the underlying optimization model is or how the changes made will affect the quality of the calculated treatment plan. This is mainly due to the fact that the medical prescription defines a set of non-linear constraints: they establish dose-volume limits that are non-linearly related with the decision variables (treatment plan parameters). This trial-and-error procedure can be very time consuming, and the final result depends on the planner's experience [8,9]. Optimization has been playing

a decisive role in improving treatment planning optimization aiming to consistently ensure high-quality plans while releasing the treatment planner for other important tasks, e.g., quality assurance. The contribution of optimization can be seen in many different aspects of radiotherapy treatment planning, from the calculation of radiation intensities [10], to the selection of appropriate irradiation angles [11–17] also considering the multiobjective nature of this problem due to the conflicting objectives to consider: maximizing CTV irradiation and, at the same time, OAR sparing [18].

The quality of a treatment plan is assessed based on a visual analysis of the three-dimensional dose distribution, on the analysis of the dosimetric parameters for each volume of interest and on the analysis of dose-volume histograms (DVH). The DVH is a graphical representation of the dose as a function of the volume, where, for each structure, the percentage of cumulative volume that receives a certain dose of radiation is obtained. Treatments are usually fractionated, meaning that a fraction of the total dose is delivered on different days. For the treatment to be delivered, the patient is positioned and immobilized on the treatment table. A mechanical arm, gantry, which rotates around a central axis, allows the radiation beam to be directed towards the patient. The treatment table can also rotate allowing, together with the rotation of the gantry, the irradiation of the tumor in almost all directions, except those where a collision between the treatment table and the gantry may occur.

Whilst treatment planning is always a difficult task for every radiotherapy treatment modality considered, it is even more difficult for IMPT due to the unavoidable impact of uncertainty. In the existing literature there are two different methodologies that try to achieve robust IMPT treatment plans: the stochastic or probabilistic approach and the worst-case scenario approach [19–21]. In the stochastic approach, a set of scenarios is usually considered, each one associated with a given probability of occurrence. The treatment planning process is then guided by an objective function that calculates a given expected value over all the considered scenarios. A probabilistic approach has been developed by Wahl et al. [22,23], considering range and setup uncertainties as random variables. In the worst-case approach, the objective is to guarantee that the best possible treatment plan for the worst possible situation is calculated [20]. This can be accomplished either by looking at the voxel, for each one of the considered structures of interest, that is in the worst situation, or looking only at the structure that, as a whole, is the worst among all the existing structures. For instance, for a given organ-at-risk (OAR) or planning OAR volumes (PRV - created by considering a given margin around the OAR), only the voxel with the highest dose contributes to the value of the objective function whilst for a clinical target volume (CTV) or planning target volume (PTV - the CTV plus a given margin) only the voxel with the lowest dose is of interest [21]. Examples of the use of the worst-case scenario can be found in Liu et al. [24] and Zaghian et al. [25].

In this work, we propose and compare two automated robust IMPT optimization approaches. The process is automated by using fuzzy inference systems, a method that has been successfully applied to intensity-modulated radiotherapy

(IMRT) [8]. These approaches differ from one another in the way uncertainty is represented and explicitly taken into consideration in the optimization. Robustness was embedded in this automated procedure considering two different strategies. The first strategy considers the creation of additional structures for each one of the volumes of interest (both CTV and OARs), named *clones*. These new structures are a copy of the original ones, but placed in a different relative position considering shifts in the x, y and z axes. All these *clones* are then taken simultaneously into account during treatment plan optimization, as well as the original ones (the number of structures that must be taken into account during treatment planning is increased). The second strategy considers one single structure for each volume of interest that is built from the union of all the corresponding *clones*. This second strategy mimics what is usually done in clinical practice: uncertainty is considered by applying margins to the CTV, creating an enlarged structure called the Planning Target Volume (PTV), and to the OARs, creating Planning Organ at Risk Volumes (PRV). These two strategies were tested on five prostate cancer cases. As uncertainty should also be explicitly considered in the assessment of the quality of the treatment plans, Monte Carlo simulation is used as an assessment tool. The different sources of uncertainty are represented by random variables, and the effects of treatment fractionation were also taken into account.

2 Sources of Uncertainty in IMPT

Any source of uncertainty in radiotherapy treatments can lead to a loss in the quality of the treatment, namely by the difference that exists between what is being planned and what is being really delivered. In IMPT, the impact of existing uncertainties is even more pronounced than in other radiotherapy modalities due to the physical properties of the beams [21]. Uncertainties can be caused by systematic errors, which are always the same in every treatment fraction, or random errors, which vary between different fractions of the treatment [6]. The greatest advantage of IMPT resides in the precise location of the Bragg peak and the respective finite range of the proton beams, but these are also the main cause of its greater sensitivity to uncertainties [20,21].

The treatment plan is based on the planning CT, where the volumes of interest are delineated. The delineation of these volumes introduces uncertainties in this process, since it is possible that different physicians perform different delineations [26]. Due to the movements of the organs and the changes that may occur during the treatment (such as the patient's weight loss, for example), this planning medical image represents only one of the possible geometries of the patient on each day of treatment. Furthermore, the artifacts that may be present in the image can influence the calculation of the depth of the Bragg peak as well as tissue density information that is given by the medical image and that impacts the calculation of the proton stopping power (uncertainties in the conversion from Hounsfield units (HU) to proton stopping power) [27]. During each fraction, in addition to internal movements of the organs, there may

be deviations in the patient's positioning on the treatment table, in relation to the position adopted in the planning CT scan. Thus, during treatment delivery, there may be changes in the beam range and Bragg peak location compared to what was planned [27], leading to an increased difficulty in adequately irradiating the tumor volume, and a potential overdose of healthy tissues [6].

Another source of uncertainty is related with the Relative biological effectiveness (RBE). RBE is a relative measure of the damage done by a given type of radiation per unit of energy deposited in biological tissues, and it is usually assumed to be equal to 1.1 for protons. However, it is known that this value should not be constant, since it depends on different factors, like proton energy, number of treatment fractions, characteristics of the traversed tissues, among others [6]. RBE uncertainties will not be considered in the current work.

3 Material and Methods

3.1 Prostate Clinical Cases

The proposed approaches were tested on five patients with prostate cancer, in stage T_2 with the tumor only present in the prostate gland, who were previously subjected to surgery. In the computer tomography (CT) images, the target volumes included the prostate gland and the CTV while the organs-at-risk considered were the rectum, bladder, right and left femoral heads. Dose prescription for the CTV was 68 Gy(RBE) to be delivered in 34 fractions. Table 1 presents the dose prescription and tolerance doses for the structures considered. In all the patients there is a significant overlap between the rectum and the CTV. Evaluation of plan quality was made using conventional dosimetric measures such as the value of the near-minimum dose, D_{98}, and the near-maximum dose, D_2, for the CTV and the mean dose and/or D_2 for the organs-at-risk. D_{98} represents the dose that is being deposited in, at least, 98% of the volume. For instance, saying that $D_{98} \geq 68$ Gy(RBE) means that at least 98% of the volume has to receive at least 68 Gy(RBE).

In the present work the irradiation angles considered were the ones usually used in clinical practice: two coplanar lateral parallel-opposed beam angles [9]. RBE was considered equal to 1.1.

Table 1. Dose prescription for the treatment plans (Gy(RBE)).

CTV	Rectum	Bladder	Femoral heads	Body
$D_{98} \geq 68$ $D_2 \leq 72.8$	$D_2 \leq 72.1$	$D_{mean} \leq 50$ $D_{max} \leq 76$	$D_2 \leq 45$	$D_{max} \leq 82$

3.2 Automated Treatment Planning Optimization

There are many different models described in the literature that can be used for treatment planning optimization when irradiation angles are considered fixed. When beam angle optimization is not performed, then the treatment parameters that must be determined consider the intensity of the radiation that is delivered from each one of the irradiation directions (beams). In IMPT these intensities can be modulated, meaning that each irradiation direction can be discretized. Each beam is interpreted as being composed by a set of small beams, the scanning pencil beams (beamlets), whose terminal zone of the beam is called a spot, responsible for the deposition of the largest dose fraction in the tumor [28]. The intensities of all the beams are optimized simultaneously, so that their spots lead to the production of a uniform total dose distribution in the tumor volume [29].

In this work, an unconstrained optimization model with a quadratic objective function was used. This objective function penalizes all voxels that do not comply with established lower and/or upper bounds. This penalty is calculated as the square difference between the upper/lower limit and the delivered dose at a given iteration, allowing to obtain a convex and easy to optimize function. This means that, for an OAR, the function is penalized when the dose at a certain voxel exceeds the corresponding upper limit, for instance. For the CTV, it is necessary to penalize the function when the dose at a given voxel is lower than the lower bound or the dose exceeds the upper bound being considered.

The objective function used for this optimization is presented in Eq. 1. The number of beamlets is represented by N and D_{ij} represents the dose contribution of beamlet j to the voxel i, so $\sum_{j=1}^{N} D_{ij}w_j$ is the total dose received by the voxel i, considering that w_j is the intensity of beamlet j. The lower and upper bounds are defined by L_s and U_s, respectively, for each structure s belonging to S, the set of all structures. Finally, λ_s is the weight (importance) of structure s.

$$\begin{aligned} \min f = & \sum_{s\in S}\sum_{i\in s}\left[\lambda_s(L_s - \sum_{j=1}^{N} D_{ij}w_j)_+^2 + (\sum_{j=1}^{N} D_{ij}w_j - U_s)_+^2\right] \\ & \text{such that}, w_j \geq 0, j = 1, \ldots, N \end{aligned} \tag{1}$$

In clinical practice, the planner iteratively changes some parameters of this objective function (namely λ_s, L_s and U_s) using a software that is called treatment planning system. The dose bounds and weights associated to each volume of interest are changed until an admissible treatment plan is found. One way to automate this process is through fuzzy inference systems (FIS), that allow an algorithmic and mathematical representation of the reasoning made by human planners during this trial-and-error procedure. FIS allow a set of simple rules to be defined, each rule of the form: if the deviation from the prescribed/tolerance dose is small, the parameters only need to be slightly changed; if the deviation from the prescribed/tolerance dose is medium, then the algorithm will need to change the parameters mediumly; if the deviation from the prescribed/tolerance dose is high, the parameters should be significantly changed. The mathematical representation of natural language concepts, like "small" or "high" can be achieved by using fuzzy numbers. This approach has already been successfully

applied to photon-based radiotherapy treatment planning in the work of Dias et al. [8], and has now been adapted to proton treatment optimization. The greatest advantage of this procedure is the fact that no manual tuning of the model parameters is needed.

3.3 Robust IMPT Treatment Planning Optimization

Two different robust automated treatment planning optimization approaches are considered and compared. In the first one, for each existing clinical region of interest (ROI - that can either be CTV or OAR) outlined by the radiation oncologist, a set of auxiliary structures is created (a set of *clones*). Each *clone* corresponds to the original structure but in a different relative position, by shifting the structure along the x, y and z axes. Overall, fourteen *clones* were created for each structure: six by shifting the original structures in each direction $(\pm x, \pm y, \pm z)$ and the remaining ones were created considering shifts in all the possible diagonal combinations. These *clones* inherit all the dosimetric objectives of the original structures, and they are all simultaneously taken into consideration during the optimization procedure to guarantee that the medical prescription is fulfilled regardless of what may occur when position and beam range uncertainties are simultaneously accounted for. Two different shift lengths were considered: 3 mm and 6 mm designated as *clones* 3 mm and *clones* 6 mm, respectively.

The second approach considers what is usually done in clinical practice, where a PTV and PRV are created as enlarged versions of the CTV and OARs to account for uncertainties. For the two alternative strategies to be fairly compared, in this work these structures are created by the union of all the corresponding *clones*. We call these structures pseudo-PTV and pseudo-PRV, just to highlight the fact that they have not been delineated manually by the medical oncologist. If manually PTV and PRV were considered, differences in the results could be due to the delineation choices and not to the differences between the two approaches. In this second approach it is possible to consider pseudo-ROI 3 mm or pseudo-ROI 6 mm, resulting from the union of the *clones* 3 mm and *clones* 6 mm, respectively.

Therefore, two robust optimization approaches were implemented: one resorting to the creation of several additional structures, the *clones*, and another one creating only one structure for each ROI, the pseudo-ROI. Both approaches were tested considering two shift lengths: 3 mm and 6 mm.

The top image of Fig. 1 shows an example of some of the *clones* created in each direction alone $(+x, +y, +z)$, for every structure. Not all the *clones* are represented in the figure as it would be impossible to distinguish the different structures in the image. Figure 1(b) shows the pseudo-PTV and pseudo-PRVs considering 6 mm shifts, as well as the original structures (but only the Pseudo-ROI structures are taken into account in treatment plan optimization).

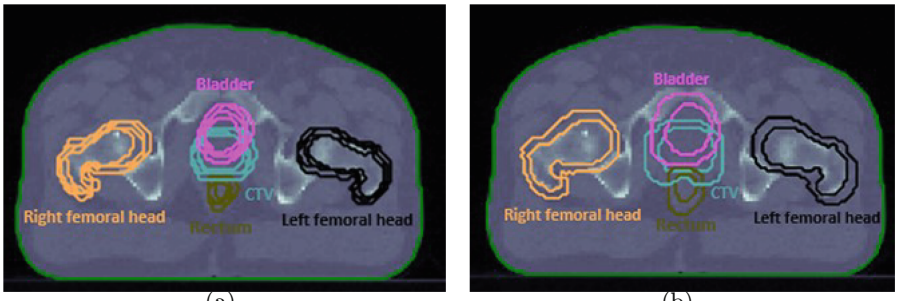

(a) (b)

Fig. 1. Representation of some of the *clones* created by applying a 6 mm shift from the structures outlined by the radiation oncologist in each direction $(+x, +y, +z)$ – 1(a) and representation of the original ROIs, as well as of the corresponding pseudo-PTV and pseudo-PRVs created from the union of all 6 mm-*clones* – 1(b).

3.4 IMPT Treatment Plan Quality Assessment

Any source of uncertainty that can arise during treatment delivery can lead to deviations between the planned and the delivered dose distribution. Thus, it is important to evaluate the resilience of each treatment plan against uncertainties. In this work, treatment plans were evaluated considering the impact of patient setup and beam range uncertainties. Monte Carlo simulation was used for this purpose, where setup and beam range uncertainties were represented by random variables following a normal distribution. In this evaluation, 100 scenarios were generated by simultaneously considering all the different sources of uncertainty, each scenario comprising 34 fractions to represent the whole treatment delivery time horizon. It is thus possible to consider both setup and random (daily) positioning errors.

Positioning uncertainties were simulated by shifting the isocenter position [30], following a normal distribution with mean of zero and a standard deviation of 2.5 mm. The positioning uncertainty considers both systematic and random errors. A random upscale or downscale was applied to the Hounsfield units of TC [20], following a normal distribution with mean value of zero and standard deviation of 1.75%. This is kept fixed for the 34 fractions. To avoid scenarios that are unlikely to occur, the maximum positioning deviation possible is 5 mm, whereas the maximum range upscale or downscale is 3.5% [25,28].

3.5 Computational Experiments Setting

The work was developed within the platform matRad, which is a radiotherapy treatment planning system developed at the German Center for Cancer Research (DKFZ) [31], programmed in MATLAB (version 2018b), for academic research. Computational tests were performed in an Intel 873 Xeon Silver 4116, 2.1 gigahertz, 12-core processor, 128 gigabyte 874 RAM.

Statistical analysis was done using the one-way ANOVA test to evaluate if there were statistical differences between the existing groups. A post-hoc Tuckey HSD test was done to confirm among which groups statistical differences occur.

4 Results

The main goal of this work was to investigate new strategies for automated robust treatment planning for IMPT. Two robust optimization approaches were applied to five prostate cancer patients. The fuzzy inference mechanism automated the FMO procedure and made it possible to achieve treatment plans complying with the defined tolerance doses and prescriptions for the defined ROI for every strategy described, i.e., the *clones* and the pseudo-ROI.

Monte Carlo simulation was used to assess the robustness of each treatment plan as well as the fulfillment of the prescribed and tolerance doses when uncertainty is explicitly considered. In this simulation, only the original structures of interest, impacted by the different sources of uncertainty, are taken into account for dose calculation.

The mean dosimetric values over the 100 scenarios were used to assess if the structure achieved or did not exceed, on average, the prescribed or tolerance dose, respectively. The standard deviation was used as a measure of robustness. The lower the standard deviation, the more robust the plan is, which means it presents a lower susceptibility to uncertainties.

For illustration purposes, the dose-volume histogram (DVH) for one of the patients in this study is presented in Fig. 2 for the plan obtained when optimization was based on the *clones* 6 mm and *clones* 3 mm strategies, for all the structures of interest, i.e., CTV, rectum, bladder, and femoral heads. The robustness of the treatment plan can be assessed by the band width of each set of curves. The narrower the set of curves the more robust the treatment plans are. For instance, the rectum is the structure where larger deviations occur, since it is the one with the widest curve group in both strategies. The curve obtained for CTV is narrower in the *clones* 6 mm strategy, compared with the *clones* 3 mm strategy, which means that there was a lower variability between the dose distributions of the CTV in the 100 simulated scenarios.

Figure 3 shows the histogram of the D_{98} values for the CTV obtained with Monte Carlo simulation for the optimization strategies implemented. The vertical dashed line indicates the prescription dose of the CTV, and thus the lowest dose value that is considered acceptable in the CTV for plan approval. This analysis is also very important because average values alone are not able to tell the whole story: for plan approval, the prescribed and tolerance doses should be met in all the generated scenarios. Monte Carlo simulation results show that, for all optimization strategies tested, the dose delivered to the CTV was equal or superior to 68 Gy(RBE) in every simulated scenario, except for the plan using *clones* 3 mm. For patient 0, the treatment plan did not achieve the prescribed dose in 12% of the scenarios (patient 0), and for other (patient 3) in 3% of the scenarios. So, the assurance of the satisfaction of the prescription under all generated scenarios was not guaranteed.

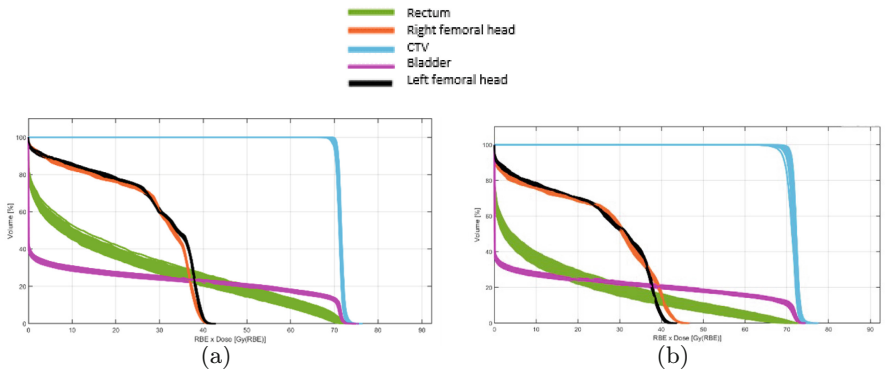

Fig. 2. DVH obtained for one patient for the 100 scenarios generated in the Monte Carlo simulation, for the strategy where *clones* were created with 6 mm shifts – 2(a) and with 3 mm shifts – 2(b) from the original structures.

Figure 4 presents a histogram with the values of D_2 for the rectum. The vertical dashed line represents the maximum dose that can be delivered to the rectum, i.e., the tolerance dose, showing that this tolerance was always respected. Furthermore, the average dose in the rectum is 5–10 Gy lower with the 3 mm shifts than with 6 mm. The bladder and right femoral head always fulfill the tolerance doses in the treatment plans calculated. Only the left femoral head exceeded the tolerance dose in the pseudo-ROI 3 mm strategy for one patient and in the pseudo-ROI 6 mm strategy in another patient.

Table 2 show the mean and standard deviation (SD) of the dosimetric parameters for the 100 scenarios simulated by Monte Carlo for each patient. The F value obtained from the ANOVA test and its p-value are also shown in Table 3, revealing that there are statistically significant differences between the four strategies.

Considering the results obtained when 3 mm shifts were used, the treatment plans obtained with the pseudo-ROI have a smaller SD than the treatment plans obtained with the *clones* 3 mm. Overall, the treatment plans obtained with the 6 mm shifted structures led to a reduction in the standard deviation comparing with the 3 mm shifts' strategies while adequate CTV coverage was achieved for every patient for the approach considering larger shifts.

For patient 0, the best CTV D_{98} value is obtained by the treatment plans *clones* 6 mm and Pseudo-ROI 3 mm, which present values that are not significantly different. Although better sparing of the rectum can be achieved, in average terms, with Pseudo-ROI 3 mm, this treatment plan is less robust since it presents a larger standard deviation value than the treatment plan based on the *clones* 6 mm strategy. A similar observation can be made regarding the right femoral head. *Clones* 6 mm present the best result for the left femoral head. For patient 1, the strategies based on the 6 mm shifts present better CTV D_{98} values, that are not significantly different between themselves. Comparing these two strategies, *clones* 6 mm present a statistically significant better OAR sparing. For

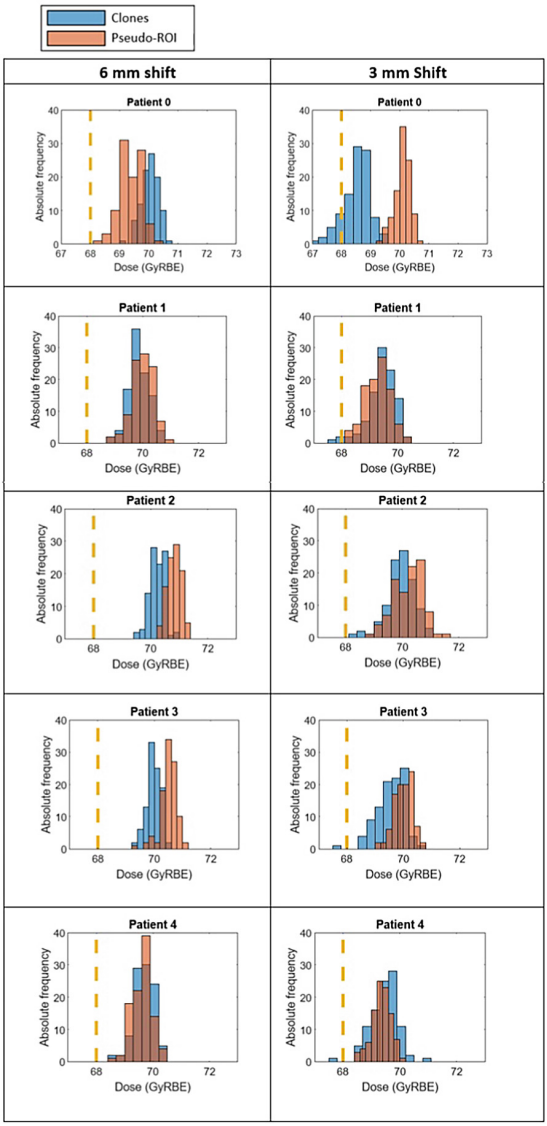

Fig. 3. Histograms of the D_{98} values for the CTV obtained with Monte Carlo simulation for the optimization strategies implemented.

patient 2, better CTV D_{98} value is obtained with the Pseudo-ROI 6 mm strategy, being the difference between this approach and the *clones* 6 mm of under 0.6 Gy. When looking at the OARs, *clones* 6 mm present much better dosimetric values, with differences, looking at the average values, of 5 Gy for femoral heads. The best CTV D_{98} value for patient 3 is also found with the Pseudo-ROI 6 mm

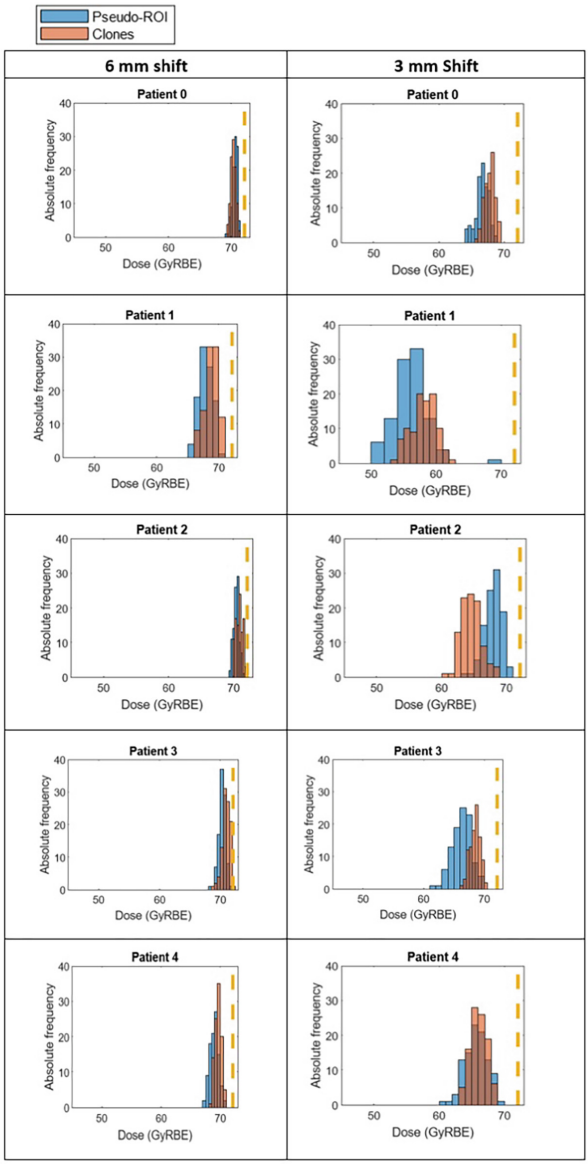

Fig. 4. Histograms of the D_2 values for the Rectum obtained with Monte Carlo simulation for the optimization strategies implemented.

strategy treatment plan but, once again, with differences considering average values of less than 0.6 Gy. *Clones* 6 mm treatment plan presents the lowest dose to the femoral heads. Pseudo-ROI 3 mm treatment plan presents a better value for rectum sparing, but at a cost of greater variability than with *clones* 6 mm.

Table 2. Mean and Standard Deviation (SD) obtained from Monte Carlo simulation, for 100 scenarios with 34 fractions, considering 3 mm and 6 mm shifts.

	3 mm shifts				6 mm shifts			
	Patient 0							
	Clones 3 mm		Pseudo-ROI 3 mm		Clones 6 mm		Pseudo-ROI 6 mm	
	Mean	SD	Mean	SD	Mean	SD	Mean	SD
D_{98} CTV	68.52^{a}	.46	70.09^{b}	.26	70.04^{b}	.29	69.38^{c}	.38
D_{mean} Bladder	11.31^{a}	.32	12.08^{b}	.31	13.61^{c}	.38	13.53^{c}	.33
D_2 rectum	66.66^{a}	.99	67.80^{b}	.78	70.56^{c}	.40	70.32^{c}	.38
D_2 right femoral head	41.09^{a}	.16	37.48^{b}	.30	39.55^{c}	.08	42.49^{d}	.08
D_2 left femoral head	41.66^{a}	.20	37.90^{b}	.21	39.92^{c}	.10	42.56^{d}	.08
	Patient 1							
	Clones 3 mm		Pseudo-ROI 3 mm		Clones 6 mm		Pseudo-ROI 6 mm	
	Mean	SD	Mean	SD	Mean	SD	Mean	SD
D_{98} CTV	69.43^{a}	.52	69.28^{a}	.47	69.84^{b}	.37	70.00^{b}	.39
D_{mean} Bladder	5.93^{a}	.30	5.75^{b}	.24	7.16^{c}	.32	8.50^{d}	.30
D_2 rectum	56.13^{a}	2.61	58.04^{b}	1.92	67.92^{c}	1.12	68.81^{d}	1.03
D_2 right femoral head	40.17^{a}	.19	39.94^{b}	.23	40.40^{c}	.29	41.13^{d}	.14
D_2 left femoral head	40.30^{a}	.29	41.38^{b}	.22	39.09^{c}	.15	42.43^{d}	.14
	Patient 2							
	Clones 3 mm		Pseudo-ROI 3 mm		Clones 6 mm		Pseudo-ROI 6 mm	
	Mean	SD	Mean	SD	Mean	SD	Mean	SD
D_{98} CTV	69.95^{a}	.50	70.21^{b}	.50	70.23^{b}	.26	70.82^{c}	.24
D_{mean} Bladder	24.94^{a}	.83	26.63^{b}	.81	30.17^{c}	.72	32.35^{d}	.66
D_2 rectum	67.98^{a}	1.29	64.58^{b}	1.51	70.44^{c}	.42	70.86^{d}	.50
D_2 right femoral head	40.96^{a}	.19	41.27^{b}	.18	39.15^{c}	.11	44.35^{d}	.23
D_2 left femoral head	41.89^{a}	.23	42.57^{b}	.34	39.45^{c}	.11	46.40^{d}	.13
	Patient 3							
	Clones 3 mm		Pseudo-ROI 3 mm		Clones 6 mm		Pseudo-ROI 6 mm	
	Mean	SD	Mean	SD	Mean	SD	Mean	SD
D_{98} CTV	69.57^{a}	.49	70.00^{b}	.32	69.97^{b}	.24	70.51^{c}	.29
D_{mean} Bladder	15.31^{a}	.29	16.42^{b}	.30	16.79^{c}	.29	17.78^{d}	.29
D_2 rectum	66.24^{a}	1.51	68.45^{b}	.83	70.32^{c}	.55	70.94^{d}	.61
D_2 right femoral head	43.21^{a}	.20	43.75^{b}	.09	39.83^{c}	.10	43.19^{a}	.20
D_2 left femoral head	40.60^{a}	.11	45.56^{b}	.08	40.16^{c}	.09	44.28^{d}	.12
	Patient 4							
	Clones 3 mm		Pseudo-ROI 3 mm		Clones 6 mm		Pseudo-ROI 6 mm	
	Mean	SD	Mean	SD	Mean	SD	Mean	SD
D_{98} CTV	69.45^{a}	.48	69.35^{a}	.33	69.68^{b}	.35	69.62^{b}	.35
D_{mean} Bladder	8.36^{a}	.55	9.53^{b}	.48	$11.47c$	.53	12.73^{d}	.68
D_2 rectum	65.69^{a}	1.72	66.16^{b}	1.22	68.97^{c}	.73	69.62^{d}	.54
D_2 right femoral head	37.54^{a}	.25	38.27^{b}	.22	39.97^{c}	.21	38.71^{d}	.18
D_2 left femoral head	36.38^{a}	.24	36.44^{a}	.32	40.29^{b}	.18	39.35^{c}	.25

Note: means with different letters are statistically different for $\alpha \leq 0.05$, considering post-hoc Tuckey HSD test. *** $p < .001$

Both *clones* 6 mm and Pseudo-ROI 6 mm present similar results regarding CTV D_{98} values for patient 4. *Clones* 6 mm spares better all the OARs but left femoral head, when compared with the Pseudo-ROI 6 mm plan.

Table 3. F values computed from the different plans calculated for each patient.

F value	Patient 0	Patient 1	Patient 2	Patient 3	Patient 4
D_{98} **CTV**	425.86***	59.27***	87.21***	121.87***	15.42***
D_{mean} **Bladder**	1125.90***	1852.61***	1959.41***	1216.47***	1185.13***
D_2 **rectum**	770.77***	1341.57***	760.36***	490.82***	294.31***
D_2 **right femoral head**	14497.24***	558.00***	13951.95***	19657.05***	2395.04***
D_2 **left femoral head**	16725.48***	4661.84***	16879.59***	67808.41***	7217.24***

Note: *** $p < .001$

5 Discussion

This paper presents and compares two different approaches for IMPT robust automated treatment plan optimization. The goal was to generate admissible treatment plans, with no human-planner intervention, guaranteeing that these plans were robust against uncertainties present in IMPT delivery, such as patient positioning and beam range. The treatment plans obtained by applying the automated fuzzy inference system optimization procedure made it possible to generate high quality plans in a totally automated way, even taking simultaneously into account a large number of structures, as it is the case with the approach based on the creation of *clones*.

Looking at the average values, and in the presence of setup and range uncertainties, the generated treatment plans can still fulfill the prescribed and tolerance doses. However, the aim was to assure that the treatment plans were admissible under all the generated scenarios and that the variability within the results was minimized. Thus, all treatment plans were assessed considering a set of 100 scenarios generated by Monte Carlo simulation.

This result is in accordance with what would be expected, but only possible thanks to the capability of the optimization method to automatically calculate treatment plans where all the restrictions (prescription and tolerance doses) are satisfied, either considering additional structures or one enlarged structure for each ROI. Actually, applying these shifts not only to the CTV but also to the OARs is crucial. If only the CTV structure was considered, then it would not be possible to properly spare the OARs when uncertainty is explicitly taken into account (actually, larger shifts would lead to worse results for the OARs).

It can be concluded that 6 mm margins increase the robustness of the treatment plans, in comparison with the 3 mm margins, guaranteeing proper CTV coverage whilst also sparing adequately OARs. Furthermore, with the treatment plans based on 6 mm shifts structures, target coverage was enhanced in comparison with the strategies using 3 mm shifts. The *clones* 3 mm strategy was the only one that did not guarantee target coverage in all the simulated scenarios. Although both strategies, i.e., the *clones* or the pseudo-ROI strategies, gave satisfactory results, some differences between them can be highlighted. The treatment plans obtained through the *clones* strategies were the ones better sparing the OARs, compared with the pseudo-ROI strategies. Actually, the *clones*

strategy with 6 mm shifts made it possible to guarantee proper target coverage while better sparing OARs in every simulated scenario.

Looking at the 6 mm shifts strategies, as target coverage was always achieved, OAR sparing and robustness of the treatment plans were the chosen features to assess which strategy performed better. The *clones* 6 mm strategy was more robust against the considered uncertainties, showing a lower standard deviation. So, these plans are less sensitive to uncertainties. Furthermore, the *clones* 6 mm delivered less dose to the OARs compared with the pseudo-ROI 6 mm. So, this strategy was able to guarantee that tolerance doses were always fulfilled. Hence, *clones* 6 mm is considered the strategy that performed best, showing a better compromise between dose prescription fulfillment and robustness.

Although these strategies were only implemented in a set of patients with prostate cancer, this study could be extended to other tumor sites. Proton radiotherapy is very sensitive to uncertainties, and even a small change in the patient's anatomy can have a large impact on the dose distribution. Consequently, a decrease in the plan's quality can occur. Hence, methods that guarantee delivery of the treatment plan to the patient as planned are crucial to further improve the success of the treatment. The strategies implemented in this study revealed that taking uncertainties into consideration during the planning process, namely considering additional auxiliary structures, led to a low variability in the dose distributions. Therefore, robust optimization algorithms can reduce the impact of uncertainties during treatment delivery.

6 Conclusion

One of the main disadvantages of Proton therapy treatment is the fact that this treatment modality is highly vulnerable to existing sources of uncertainty. This can lead to significant differences between the treatment that is planned and the treatment that is indeed delivered, with consequences in terms of the treatment outcome (probability of disease control and of occurrence of treatment induced complications). In this paper we show that explicitly taken uncertainty into account when optimizing treatment plans can improve the robustness of the treatment plans without increasing the workload of the human planners, since all the process can be totally automated. Robust optimization methods contribute to reducing the impact of setup and range uncertainties in the treatment plan for IMPT. Robust treatment plans were achieved with the four different strategies, i.e., the *clones* and pseudo-ROIs created with two different shift lengths. This conclusion can be reached since the fulfillment of the prescribed and tolerance doses was accomplished in almost every scenario (being the exception the *clones* 3 mm strategy). Most importantly, the robustness is assessed by the low standard deviations obtained, that reveal a low variability in the dose distributions. The difference between each one of the implemented strategies is related to compromises that exist among OAR sparing, tumor coverage and robustness. It was shown that the *clones* were better at guaranteeing these compromises compared to the pseudo-ROI's strategies.

It can be concluded that the *clones* 6 mm strategy can be a valuable alternative, assuring the automatic calculation of robust treatment plans that behave well under uncertainty. This strategy shows benefits when compared with the consideration of a single enlarged structure for each ROI (similar to the PTV/PVR approach). As the number of structures that are simultaneously considered increases significantly, this strategy is only feasible due to the possibility of using FIS to automate treatment planning optimization.

Acknowledgments. This work has been partly supported by the Fundação para a Ciëncia e a Tecnologia (FCT) under project grants UTA-EXPL/FMT/0079/2019, UIDB/00645/2020, UIDB/00308/2020 and UIDB/05037/2020 with DOI 10.54499/UIDB/05037/2020.

References

1. Evans, E., Staffurth, J.: Principles of cancer treatment by radiotherapy. Surg. Oxf. **36**, 111–116 (2018)
2. Shepard, D.M., Ferris, M.C., Olivera, G.H., Mackie, T.R.: Optimizing the delivery of radiation therapy to cancer patients. SIAM Rev. **41**, 721–744 (1999)
3. Brady, L.W., Heilmann, H.P., Molls, M.: New Technologies in Radiation Oncology. Springer, Heidelberg (2006). https://doi.org/10.1007/3-540-29999-8
4. Song, J., Shi, Z., Sun, B., Shi, L.: Treatment planning for volumetric-modulated arc therapy: Model and heuristic algorithms. IEEE Trans. Autom. Sci. Eng. **12**, 116–126 (2014)
5. Wang, F., Huang, Y.-L., Ju, F.: Simulation optimization gantry call-back control method for proton therapy systems. IEEE Trans. Autom. Sci. Eng. **20**, 1565–1576 (2022)
6. Mohan, R., Grosshans, D.: Proton therapy-present and future. Adv. Drug Deliv. Rev. **109**, 26–44 (2017)
7. ICRU, Prescibing, Recording and Reporting Proton-Beam Therapy (ICRU Report 78). J. ICRU (2007)
8. Dias, J., Rocha, H., Ventura, T., Ferreira, B., Lopes, M.C.: Automated fluence map optimization based on fuzzy inference systems. Med. Phys. **43**, 1083–1095 (2016)
9. Cao, W., et al.: Reflections on beam configuration optimization for intensity-modulated proton therapy. Phys. Med. Biol. **67**, 13TR01 (2022)
10. Rocha, H., Dias, J.M., Ferreira, B.C., Lopes, M.C.: Combinatorial optimization for an improved transition from fluence optimization to fluence delivery in IMRT treatment planning. Optimization **61**, 969–987 (2012)
11. Lim, G.J., Cao, W.: A two-phase method for selecting IMRT treatment beam angles: branch-and-Prune and local neighborhood search. Eur. J. Oper. Res. **217**, 609–618 (2012)
12. Bertsimas, D., Cacchiani, V., Craft, D., Nohadani, O.: A hybrid approach to beam angle optimization in intensity-modulated radiation therapy. Comput. Oper. Res. **40**, 2187–2197 (2013)
13. Rocha, H., Dias, J.M., Ferreira, B.C., Lopes, M.C.: Selection of intensity modulated radiation therapy treatment beam directions using radial basis functions within a pattern search methods framework. J. Glob. Optim. **57**, 1065–1089 (2013)

14. Dias, J., Rocha, H., Ferreira, B., Lopes, M.C.: A genetic algorithm with neural network fitness function evaluation for IMRT beam angle optimization. Cent. Eur. J. Oper. Res. **22**, 431–455 (2014)
15. Lim, G.J., Kardar, L., Cao, W.: A hybrid framework for optimizing beam angles in radiation therapy planning. Ann. Oper. Res. **217**, 357–383 (2014)
16. Rocha, H., Dias, J.M., Ventura, T., Ferreira, B.C., Lopes, M.C.: Beam angle optimization in IMRT: are we really optimizing what matters? Int. Trans. Oper. Res. **26**, 908–928 (2019)
17. Gutierrez, M., Cabrera-Guerrero, G., Lagos, C.: A Reduced Variable Neighbourhood Search for the Beam Angle Optimisation Problem. IEEE Trans. Emerg. Top. Comput. Intell. **7**, 1499–1510 (2023)
18. Chan, T.C., Craig, T., Lee, T., Sharpe, M.B.: Generalized inverse multiobjective optimization with application to cancer therapy. Oper. Res. **62**, 680–695 (2014)
19. Wedenberg, M., Beltran, C., Mairani, A., Alber, M.: Advanced treatment planning. Med. Phys. **45**, e1011–e1023 (2018)
20. Unkelbach, J., Paganetti, H.: Robust proton treatment planning: physical and biological optimization. Semin. Radiat. Oncol. **28**, 88–96 (2018)
21. McGowan, S.E., Burnet, N.G., Lomax, A.J.: Treatment planning optimisation in proton therapy. Br. J. Radiol. **86**, 20120288–20120288 (2013)
22. Wahl, N., Hennig, P., Wieser, H.P., Bangert, M.: Efficiency of analytical and sampling-based uncertainty propagation in intensity-modulated proton therapy. Phys. Med. Biol. **62**, 5790 (2017)
23. Wahl, N., Hennig, P., Wieser, H.-P., Bangert, M.: Analytical incorporation of fractionation effects in probabilistic treatment planning for intensity-modulated proton therapy. Med. Phys. **45**, 1317–1328 (2018)
24. Liu, W., et al.: Effectiveness of robust optimization in intensity-modulated proton therapy planning for head and neck cancers. Med. Phys. **40**, 051711 (2013)
25. Zaghian, M., Cao, W., Liu, W., Kardar, L., Randeniya, S., Mohan, R., Lim, G.: Comparison of linear and nonlinear programming approaches for "worst case dose" and "minmax" robust optimization of intensity-modulated proton therapy dose distributions. J. Appl. Clin. Med. Phys. **18**, 15–25 (2017)
26. Khoo, E.L., et al.: Prostate contouring variation: can it be fixed? Int. J. Radiat. Oncol. Biol. Phys. **82**, 1923–1929 (2012)
27. Unkelbach, J., et al.: Robust radiotherapy planning. Phys. Med. Biol. **63**, 22TR02 (2018)
28. Liu, W., Zhang, X., Li, Y., Mohan, R.: Robust optimization of intensity modulated proton therapy. Med. Phys. **39**, 1079–1091 (2012)
29. Mohan, R., Das, I.J., Ling, C.C.: Empowering intensity modulated proton therapy through physics and technology: an overview. Int. J. Radiat. Oncol. Biol. Phys. **99**, 304–316 (2017)
30. Fredriksson, A., Forsgren, A., Hardemark, B.: Minimax optimization for handling range and setup uncertainties in proton therapy. Med. Phys. **38**, 1672–1684 (2011)
31. Wieser, H.P., et al.: Development of the open-source dose calculation and optimization toolkit matRad. Med. Phys. **44**, 2556–2568 (2017)